Tropopause Detected by Radar

Abstract. *The tropopause has been detected by ultrasensitive, narrow-beam, microwave (10.7-centimeter) and ultrahigh-frequency (71.5-cm) radars. Its reflectivity is consistent with that expected theoretically for a refractively turbulent medium. Indications are that the layer is also mechanically turbulent, and that electromagnetic scatter techniques may be used to detect high-altitude clear-air turbulence.*

The tropopause, the level marking the upper boundary of the troposphere and the lower limit of the stratosphere, has been detected by two of three ultrasensitive radars at Wallops Island, Virginia (*1*). To our knowledge this is the first such report from the western world; Zhupakhin (*2*) recently reported detection from the Soviet Union, but with few details.

Our work is part of a long-range program of study of the nature of the electromagnetic scatter from the clear atmosphere, directed toward (i) understanding the long-mysterious radar "angel" echoes from invisible targets, (ii) knowledge of the mechanisms of scatter propagation beyond the horizon, and (iii) determining the extent to which powerful radars may be used to probe the atmosphere. In particular we seek to determine whether or not radar and forward-scatter techniques may be used to detect high-altitude clear-air turbulence. An earlier report (*3*) on clear-air radar echoes in the lower troposphere showed that echo layers may be associated with scatter from a refractively turbulent stratum in the atmosphere or with insects.

The radars operate at wavelengths of 3.2, 10.7, and 71.5 cm from circular paraboloidal antennas of 10.4-, 18.3-, and 18.3-m diameters, respectively; the corresponding beam width are 0.2, 0.48, and 2.9 deg, respectively. The most important overall system parameter is the minimum detectable reflectivity, η_{min}: 2.8×10^{-16} cm^{-1} at 3.2 cm, 8.5×10^{-18} cm^{-1} at 10.7 cm, and 7×10^{-19} cm^{-1} at 71.5 cm, all at a target range of 10 km. These values include the effect of enhanced detectability resulting from integration on the face of the scope and the film when the beams are scanned slowly in elevation at a rate of 2.5 deg/sec.

Figure 1 shows three simultaneous photographs of the range-height indicators of the three radars, taken while the beams were scanning synchronously in elevation angle at an azimuth of 90 deg. The top photo (X-band, 3.2 cm), shows a cirrostratus (ice-crystal) cloud based at about 7 km, with its top at about 11 km. The middle photo (S-band, 10.7 cm), shows the same cloud mass, although its top extends only to 10 km; this is to be expected because the 3.2-cm radar is slightly more sensitive than the 10.7-cm radar (by 5.85 db, or a factor of 3.85) with clouds whose particles are much smaller than the wavelength (that is, Rayleigh scatterers). This is to say that, while the minimum detectable reflectivity of the 10.7-cm radar is better (less) than that of the 3.2-cm radar by a factor of 32.4, the cloud reflectivity is greater at 3.2 cm by a factor of 125 (that is, the 4th power of the wavelength ratio). The net effect is a 5.8-db advantage at 3.2 cm for clouds and precipitation, so that this radar detects the weaker tops of the cirrostratus cloud.

However, the 10.7-cm photo (S-band) also shows a weak but definite echo layer at 12-km altitude where the 3.2-cm photo shows nothing. Clearly this difference could not be caused by clouds, dust, or particulates of any kind, since such targets would have been detected more strongly at 3.2 cm. The 12-km-high echo layer extends to

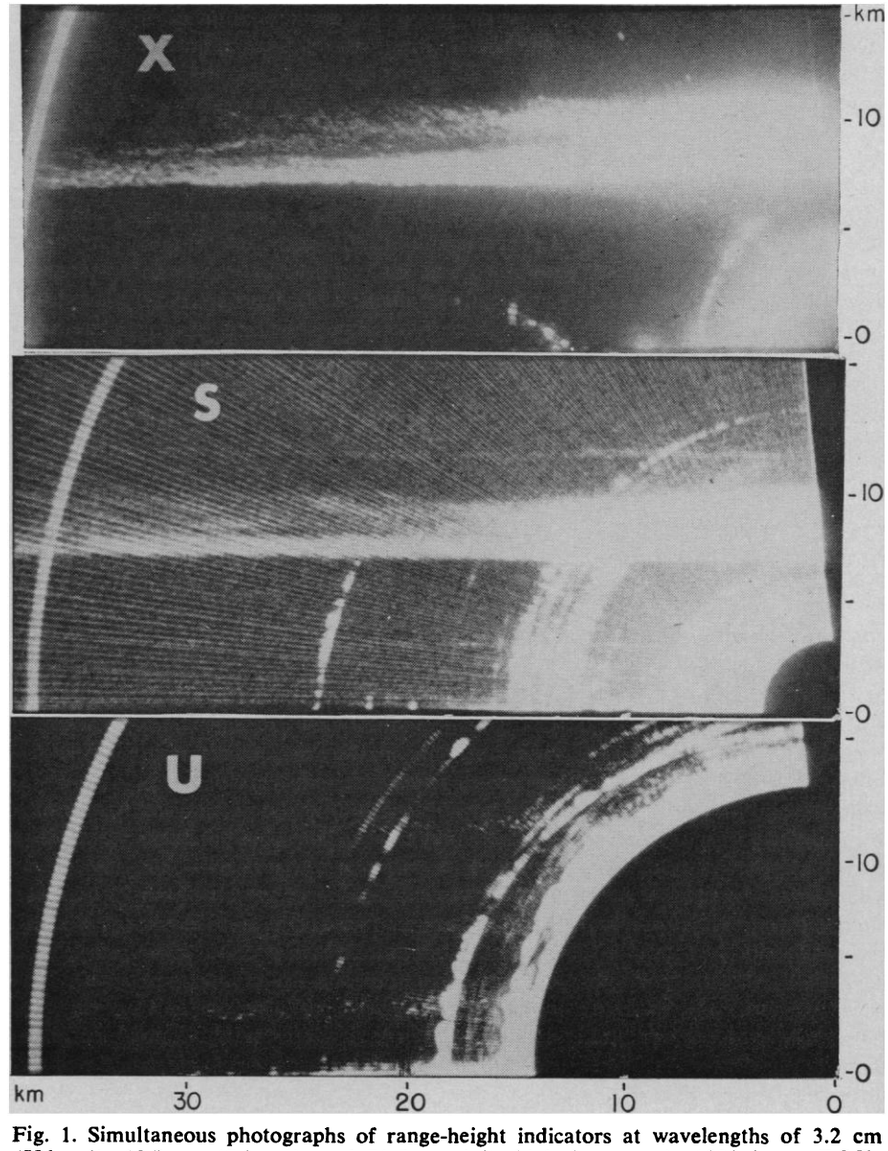

Fig. 1. Simultaneous photographs of range-height indicators at wavelengths of 3.2 cm (X-band), 10.7 cm (S-band), and 71.5 cm (ultrahigh frequency); 1030 hours E.S.T., 18 February 1966, at Wallops Island, Va.; azimuth, 90 deg. Because of the printing process, the echo layer at 12 km does not appear in the bottom photograph.

a range of 30 km (discernable in the original photo), where it fades into the background noise; if one assumes that it is horizontally homogenous, the corresponding 10.7-cm-layer reflectivity is 7.7×10^{-17} cm^{-1}.

The radiosonde ascent at 1300 E.S.T. from Wallops Island showed a well defined tropopause at 11.6 km, just below the height of the 10.7-cm echo layer; this finding suggests association between echo layer and tropopause. Similar correspondence on five other occasions (7, 21, and 28 February; 15 March; and 4 April 1966) indicates that we are in fact detecting some refractive index structure at or near the tropopause.

For better understanding of the scatter mechanism, we now refer to the 71.5-cm photo (bottom). Because of its long wavelength, this radar fails to detect the cloud at all. But the echo layer at 12 km is again detected, this time to a range of 28 km. The corresponding layer reflectivity is 2 to 3 $\times$ 10^{-17} cm^{-1}, when one considers that the large beam of this radar is about 20- to 25-percent filled by the layer of 250-m depth, as estimated from the 10.7 cm photo. Thus our best estimate indicates that the 10.7-cm reflectivity is about 2 to 4 times as great as that at 71.5-cm wavelength.

According to Tatarski (*4*), the radar reflectivity of a region of isotropic homogeneous turbulence in refractive index is

$$\eta = 0.39\, C_n^2 \lambda^{-\frac{1}{3}} \qquad (1)$$

where λ is wavelength, C_n^2 being a coefficient defined by

$$C_n^2 = 5.26\, \overline{(\Delta n)^2}\, L_o^{-\frac{2}{3}} \qquad (2)$$

where $\overline{(\Delta n)^2}$ is the mean-square fluctuation in refractive index as a function of distance, and L_o is the large-scale limit of the turbulence spectrum. According to Eq. 1, the reflectivity of such a medium should decrease slowly with increasing wavelength: from 10.7- to 71.5-cm wavelength it should decrease by a factor of 1.84, compared with our experimental finding of 2 to 4; the agreement is within the experimental errors. Similar reflectivity ratios were measured on four of the five other occasions; one instance, showing significantly greater reflectivity at 71.5 cm than at 10.7 cm, may correspond to a turbulence spectrum slightly different from that assumed by Tatarski (see *4*).

We conclude that the echo layer in question results from back-scatter from a refractively turbulent medium. Using the measured 10.7-cm reflectivity of 7.7×10^{-17} cm^{-1} in Eq. 1, we find

$$C_n^2 = 4.4 \times 10^{-16}\ \text{cm}^{-\frac{2}{3}} \qquad (3)$$

This value is to be compared to the range of 10^{-16} to 10^{-14} cm$^{-\frac{2}{3}}$ estimated theoretically by Atlas *et al.* (*5*) for regions of high-altitude clear-air turbulence. Thus both the magnitude of the echoes and their wavelength dependence are in reasonable accord with our hypothesis.

Calculating the theoretically expected reflectivity at 3.2-cm wavelength according to Eq. 1, we find that it should be 1.5 times the 10.7-cm reflectivity, or 1.2×10^{-16} cm^{-1}—which is about 25 percent of the minimum detectable reflectivity of the 3.2-cm radar at a range of 12 km, so that this radar should not have detected the layer even when pointing vertically. Of course this is what we found. One should note, however, that Eq. 1 is not completely valid at wavelengths shorter than about 5 cm (*5*). This problem is more comprehensively treated elsewhere (*1*).

So far we have referred only to echoes associated with a "refractively" turbulent medium, since it is the fluctuations in refractive index that cause the scatter. What then can we say about the "mechanical" turbulence? Eqs. 1 and 2 show that the radar reflectivity is proportional to the mean-square refractivity fluctuation $\overline{(\Delta n)^2}$. Tatarski (*4*) shows that this is proportional to $(ML_o)^2$, where M is the vertical gradient of refractivity and L_o is the outer (large)-scale limit of the turbulence spectrum. Other things being equal, L_o is a measure of the intensity of mechanical turbulence. In other words, at a layer of sharp vertical gradient of refractivity (that is, large M), the atmosphere needs to be perturbed only slightly (small L_o) for it to cause a significant refractivity fluctuation. In the lower atmosphere, where moisture is dominant in determining the microwave refractivity of the air, one may find exceedingly large M's, especially at sharp subsidence and low-level nocturnal inversions; in such instances the mechanical turbulence or displacement (L_o) can be quite small and still provide sufficiently large refractivity perturbations to be detectable. On the other hand, high in the troposphere and at the tropopause, M is considerably smaller than at the lower levels; in this case, L_o must be quite large (of the order of 100 m or greater) for it to provide equally large $\overline{(\Delta n)^2}$.

The reasoning (*1*) is somewhat more complex than our treatment implies. However, the result is that considerations of C_n^2 (the reflectivity coefficient in Eq. 1) and L_o, along with the vertical wind shear at the tropopause, indicate that a 10.7-cm-wavelength reflectivity such as we have reported must be associated with "moderate" clear-air turbulence on the quantitative scale of MacCready *et al.* (*6*). Moreover, the minimum detectable reflectivity at 10.7 cm (and 10-km range) corresponds to light-to-moderate clear-air turbulence on the referenced scale. The implication is that the detection of a clear-air stratum at high altitudes by radars such as those at Wallops Island is a sign of some degree of hazardous clear-air turbulence. Unfortunately, we have yet to obtain direct confirmation of this thesis from high-flying aircraft.

We hasten to add that this does not mean that radars such as ours provide a practicable means of detecting clear-air turbulence. Indeed, at best we have detected the tropopause to a range of only 30 km. Thus it would not be economically feasible to cover the nation's airways with such powerful radars with 50- or 60-km spacing. However, we note that when microwaves are scattered so well in the backward direction the forward-scatter is many times larger; indeed, it can be shown (*5*) that the reflectivity for forward-scatter (η_f) is related to that for back-scatter (η_b) approximately by

$$\eta_f \simeq \eta_b / [\sin^{11/3}(\theta/2)] \qquad (4)$$

where θ is the angle between the transmitter and receiver beams oriented to intersect at the scattering layer. For regions at altitudes of the order of 10 km, with a spacing of 100 to 200 km between transmitter and receiver, the forward-scatter reflectivity would be 100 to 10,000 times as great as that in the radar direction. Extensive calculations (*7*) demonstrate that forward-scatter techniques would indeed provide the basis of a practicable clear air–turbulence detection system.

DAVID ATLAS
KENNETH R. HARDY
KENNETH M. GLOVER
Air Force Cambridge Research Laboratories, Bedford, Massachusetts
ISADORE KATZ
THOMAS G. KONRAD
Applied Physics Laboratory, Johns Hopkins University, Baltimore, Maryland

References and Notes

1. D. Atlas, K. R. Hardy, T. G. Konrad, *Proc. Weather Radar Conf. 12th* (Amer. Meteorol. Soc., Boston, in preparation).
2. K. S. Zhupakhin, *Glavnaia Geofiz. Observ. Tr. No. 177*, p. 129 (1965) [*Res. transl. TR-629* (Air Force Cambridge Res. Labs., Bedford, Mass., 1966)].
3. K. R. Hardy, D. Atlas, K. M. Glover, *J. Geophys. Res.* **71**, 1537 (1966).
4. V. I. Tatarski, *Wave Propagation in a Turbulent Medium* (McGraw-Hill, New York, 1961).
5. D. Atlas, K. R. Hardy, K. Naito, *J. Appl. Meteorol.*, in press.
6. P. B. MacCready, Jr., R. E. Williamson, S. Berman, A. Webster, "Operational application of a universal turbulence measuring system," *NASA Rept. CR-62025* (Meteorology Research, Inc., Altadena, Calif., 1965).
7. D. Atlas and K. Naito, *Proc. Weather Radar Conf. 12th* (Amer. Meteorol. Soc., Boston, in preparation).

8. Work supported by the laboratory director's fund, Air Force Cambridge Research Laboratories, and by NASA. We thank Jack Howard, Wallops Island, and his staff for their assistance.

22 June 1966

Mercury: Infrared Evidence for Nonsynchronous Rotation

Abstract. *An infrared observation of the dark side of Mercury made by Pettit and Nicholson in 1923 led them to suggest that the planet rotates nonsynchronously. Their early measurements, if taken at face value, would imply a brightness temperature of about 180°K for the dark side. The asymmetry of the infrared phase curve is further interpreted as suggesting direct rotation.*

Radar observations at the Arecibo Ionospheric Observatory by Pettengill and Dyce (*1*) indicate that Mercury rotates with a direct nonsynchronous period of 59 ± 5 days. Peale and Gold (*2*) showed that this could have been theoretically expected as a consequence of solar tidal torque acting along an eccentric orbit.

Pettit and Nicholson (*3*) reported an observation of Mercury which they correctly interpreted as indicating nonsynchronous rotation. The observation was probably made on 21 June 1923, with an infrared-sensitive (*8–14* μ) thermocouple receiver at the focus of the 100-inch (2.5 m) Mt. Wilson reflector. The phase angle i (the planetocentric angle between Earth and Sun) and fractional illumination k of the planet were about 110°W and 0.32, respectively. The diameter of the planetary image was 0.55 mm, while that of the thermocouple receiver was 0.40 mm.

The authors had no absolute calibration at the time, but measured only a deflection from the thermocouple. The receiver was centered on the illuminated crescent, giving a maximum free deflection of 132.2 mm, the crescent intersecting 50 percent of the receiver. The receiver was moved close to the convex limb of the crescent (position A in Figure 1) and a deflection of 1.5 mm was obtained as a dark sky reading. But when the receiver was brought to the same distance from the terminator, approaching from the darkened side (position B), a deflection of 4.0 mm was obtained.

However, if the rotation of Mercury were synchronous, the thermal emission from the dark side would have been near the detection threshold of the thermocouple and should have caused about the same deflection as the dark sky reading at position A. But in fact the deflection for position B was greater, and the investigators suggested that "any radiation from the dark side of Mercury is an indication of a short rotation period. . . ."

Subsequently, Antoniadi (*4*) and others, using extensive optical observations of Mercury, reestablished the older view that the planet rotated in synchronism with the sun, and the scientific community was generally convinced. Apparently no one thereafter sought thermocouple data for the dark-side of Mercury.

Pettit and Nicholson (*5*) later developed a system of absolute calibration, from which it could be determined that the total energy (E) radiated from Mercury and arriving outside Earth's atmosphere on 21 June 1923, was $E = 218 \times 10^{-12}$ cal cm^{-2} min^{-1}, normalized for the planet at mean distance from the sun and at one astronomical unit from the earth. This value was based on observations with a larger thermocouple receiver that covered the entire disk of Mercury, but it can be used here to derive an approximate value for the brightness temperature of the dark side. First, recalling the 1.5-mm dark-sky reading, we define an "effective deflection"

$$D = (d - 1.5)/f$$

where d is the observed deflection in millimeters and f is the fraction of the thermocouple receiver actually used to measure the region of interest. The illuminated crescent, the dark portion, and the entire disk of the planet may be designated by subscripts 1, 2, and 3, respectively. We then have $d_1 = 132.2$, $d_2 = 4.0$, $f_1 = 0.50$, and

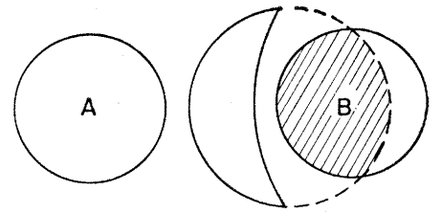

Fig. 1. Positioning of infrared receiver with respect to crescent of Mercury by Pettit and Nicholson (*3*). Dark sky observed at A and portion (*shaded*) of unilluminated hemisphere at B.

(as may be shown, with $k = 0.32$ together with the relative areas of the planetary and thermocouple disks) $f_2 \approx 0.75$ (that is, the shaded portion of region B in Fig. 1). Therefore $D_1 = 261.4$ and $D_2 \approx 3.3$. The effective deflection corresponding to the entire disk is

$$D_3 = kD_1 + (1 - k)D_2 = 85.8$$

The surface brightness temperature T_3, which corresponds to this deflection, can be computed from the normalized radiant energy E received from the entire planet according to

$$E = \sigma R^2 T_3^4$$

where σ is the Stefan-Boltzmann constant and R is the radius of Mercury in astronomical units. With unit emissivity, the result is $T_3 = 316$°K.

Knowledge of the mean temperature corresponding to D_3 now allows a determination of the dark side surface temperature responsible for D_2. The effective deflection is proportional to that part of the blackbody energy which penetrates the earth's atmosphere, and thus depends upon the temperature of the radiating surface according to

$$D(T) = S \int_{3\mu}^{24\mu} B_\lambda(T)\, E_\lambda\, d\lambda$$

where $B_\lambda(T)$ and E_λ are, respectively, the blackbody intensity due to a surface at temperature T and the atmospheric transmissivity at wavelength λ. The constant S is characteristic of the detecting apparatus; its response is assumed to be uniform over the relevant range of wavelengths. The integration need not be over all wavelengths since B_λ (316°K) essentially vanishes for $\lambda < 3\mu$.

The major part of planetary thermal radiation comes through the 8 to 14 μ window, and the E_λ curve used for this range is that of Sinton and Strong